Int. J. Nano Dimens., 14 (4): 348-355, Autumn 2023

ORIGINAL ARTICLE

Synthesis, characteristics, and photocatalyst effect of nAF and $ZnAl_2O_3/AlF_3$ nanocomposite with sol-gel method

Elinaz Ahmadian [1], Maryam Kargar Razi [1,], Babak Sadeghi [2], Mahbobeh Nakhaei [1]*

[1] *Department of Chemistry, Islamic Azad University, North Tehran Branch, Tehran, IRAN*
[2] *Department of Chemistry, Islamic Azad University, Tonekabon Branch, Tonekabon, IRAN*

Received 01 July 2023; revised 25 August 2023; accepted 28 August 2023; available online 02 September 2023

Abstract

In this framework study, an attempt was made to synthesize, characterize, and develop some applications of nano AlF_3 (nAF) by sol-gel method. Meanwhile, precursor gel preparation and the interaction on the nano-sized area have been studied. By nAF the $ZnAl_2O_3/AlF_3$ (ZA) nanocomposite has been successfully prepared and Structural, morphological and thermal characterization has been done using by FT-IR, XRD, SEM, TG-DTG, and HRTEM techniques. This nanocomposite was used for the removal of Congo red dye. For this purpose, the morphology and the structure of crystals has been changed by modification on precursor gel. When precursor gel has been changed from 4 to 9 h, the size of crystals decreased to 15-20 nanometers. The results showed that ZA have been efficiency for photocatalysts in decolorization of Congo red.

Keywords: *Activity of Catalist; Condo red; Nano AlF_3; Poly Vinyl Choloride; Sol-gel; XRD.*

How to cite this article

Ahmadian E., Kargar Razi M., Sadeghi B., Nakhaei M. Synthesis, characteristics, and photocatalyst effect of nAF and $ZnAl_2O_3/AlF_3$ nanocomposite with sol-gel method. Int. J. Nano Dimens., 2023; 14(4): 348-355.

INTRODUCTION

Now pure or organic-inorganic hybrid materials and Nano-metal oxides, are applied and available from synthesis of the sol-gel method [1-2]. Zinc oxide has been long studied to degradation and decolorization of Congo red dye [3, 4]. Therefore, ZnO doping with metal or non-metals can improve its photocatalytic activity in the visible light region [5]. One of the most practical materials in recent times for researchers is Aluminum Fluoride nanoparticles (nAF). Their excellent properties, e.g., ease in the manipulation of fabrication, high specific surface area, and etc. is reported [6, 7]. Degradation of Congo red dye by a Fe_2O_3-CeO_2-ZrO_2/palygorskite composite catalyst was studied by Ouyang and the result indicated that the adsorption efficiency of CR was up to 95% [8].

On the catalyst's performance in sol-gel processes has been significance many factors of the catalyst condition, such as raw materials, temperature, pH. Several of current and potential applications for Aluminum fluoride have as an increase the electrical conductivity and to lower the melting point [9-14]. Moreover, AlF_3 is one of the most critical catalysts for exchange reactions in the supports halogens [15-18]. Sol-gel method, sputtering and chemical vapor deposition are some of methods have been applied for the synthesized of $nAlF_3$ thin films, which the sol-gel method is the most widely used.

We have recently developed a reduction method of converting Ag nanospheres into nanorods [19], nanoplates [20], their antibacterial activity [21, 22], an improved an easy synthetic route for silver nanoparticles in poly (diallyldimethylammonium chloride) (PDDA) [23], synthesis of Gold/HPC hybrid nanocomposite [24], Preparation of Ag/ZnO nanocomposite [25, 26] and comparison nanosilver particles and nanosilver plates for the oxidation of ascorbic acid [27].

We have been synthesized $ZnAl_2O_4/AlF_3$ (ZA) nanocomposite by using the sol-gel method. The produce of ZA nanocomposite by using a

* Corresponding Author Email: *mkargarrazi@yahoo.com*

Table 1. Analysis of the synthesized crystal.

SiO_2	0.02
Fe_2O_3	0.02
Na_2O	0.01
P_2O_5	0.005
SO_4^{2-}	-
$\%AlF_3$	95%
L.O.I	0.85%
Humidity	0.1%
Bulk density	0.7 Kg/dm^3

hybrid sol–gel combustion method at relatively low temperature is a new method, especially applied to form of photocatalyst. Degradation photocatalytic process under UV light radiation showed high decomposition of congo-red dye in a short time (98.9% - 75 min).

EXPERIMENTAL

Characterization

In this investigation, a FESEM (SNE 4500-M) equipped with an energy dispersive X-ray spectrometer (EDS) was used to assess coating morphology. Structural properties of the composite film were carried out using a Broker-based D8-Advance device detector, the XRD measurements were performed. The analyses were carried out at all angles of 2θ, from 3° to 80°, with steps of 0.1°, a stoppage time of 0.1 seconds per step at room temperature, and a pressure of 1 atm. The FT-IR spectra were recorded using KBr discs and Nujol in the wavelength range 400-4000 cm^{-1} on FT-IR (Model Perkin–Elmer). TG-DTG analysis with radiation of Cu-Kα in the range 10º–80º (2θ) was recorded using Bruker AXS diffractometer D8 ADVANCE. Using a UV-1800, a UV-Vis spectrophotometer investigated the optical properties of samples.

Materials and methods

All of the materials are laboratory-grade and have been purchased from Merck Company. The nAF with the addition of ($Al(CH_3COO)_3$) was started the reaction and finished by adding of HF solution. pH of solution was changed between 7 and 10. The Ammonium solution, 0.50 g $nAlF_3$ and 0.06 g Zinc choloride·$4H_2O$ (in 15 mL water) added, then mixed for 30 min at 45 ºC. The white precipitates ZA were filtered and dried at room temperature for three days. The most experimental details are summarized in Table 1.

RESULT AND DISCUSSION

The precipitant in this sample was nAF. The crystalline shape of nAF, has been observed in the XRD pattern [15, 16] in during the reaction 1.

$$\mathrm{Al(CH_3COO)_3 + Al_2O_2F_4 + 5HF \xrightarrow[\text{In glass reactor}]{\text{alkaline regions}} 3nanoAlF_3 + (nAF)}$$

$$\mathrm{3\ CH_3COOH + H_2 + O_2 \quad (NH_3\ Solvent)} \qquad (1)$$

The conforming XRD pattern is reported in Fig. 1. The X-ray diffraction (XRD) analysis of the as prepared nAF was carried out for investigate the structural properties. The appearance intensity of peaks (weak and broad peaks) in the XRD pattern indicates that the particle size is small. The nature of the synthesized samples indicates with the broadening of the diffraction peaks nanostructure. The peaks of nAF at 2θ of 25.1°, 35.2°, 42.7°, 52.3°, and 58.5° are assigned to the (111), (200), (220), (311), and (222), respectively. The orthorhombic structure has been provided (reaction 1) for crystal planes of nAF (JCPDS-No. 83-2384) [28-31]. The XRD patterns showing that the nAF sample nano area is successfully synthesized. The crystal size with using the Scherrer equation for sample was 15.6 nm.

TEM analysis shows that morphology of nAF is in nano area. The synthesized nAF with the regular shape has spherical shape structure and has been connected to each other. The spherical structure can has numerous abilities and the size and shape of the nanoparticles affects the properties such as rheology, stability, and optical characteristics. The size of the particle in the HRTEM is in the range 15-20 nm which as it matches the XRD patterns (Figs. 2a, 2b).

In the formed alumina precipitates has been displayed that variation between two samples

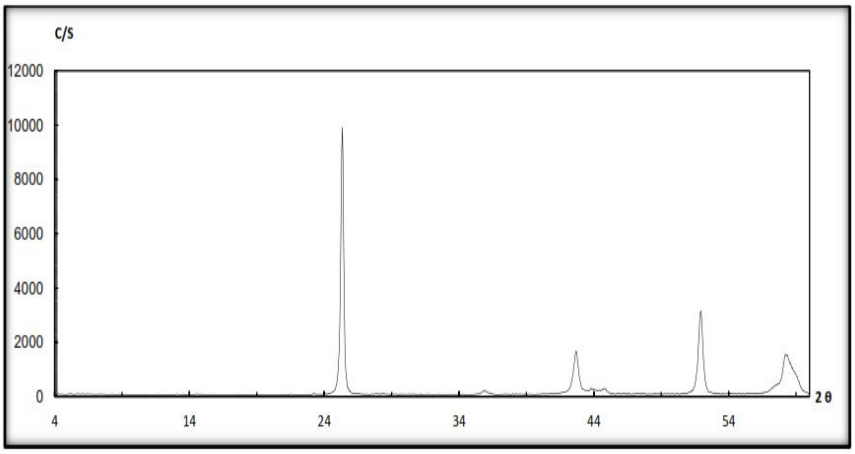

Fig. 1. The XRD pattern of the nAF sample.

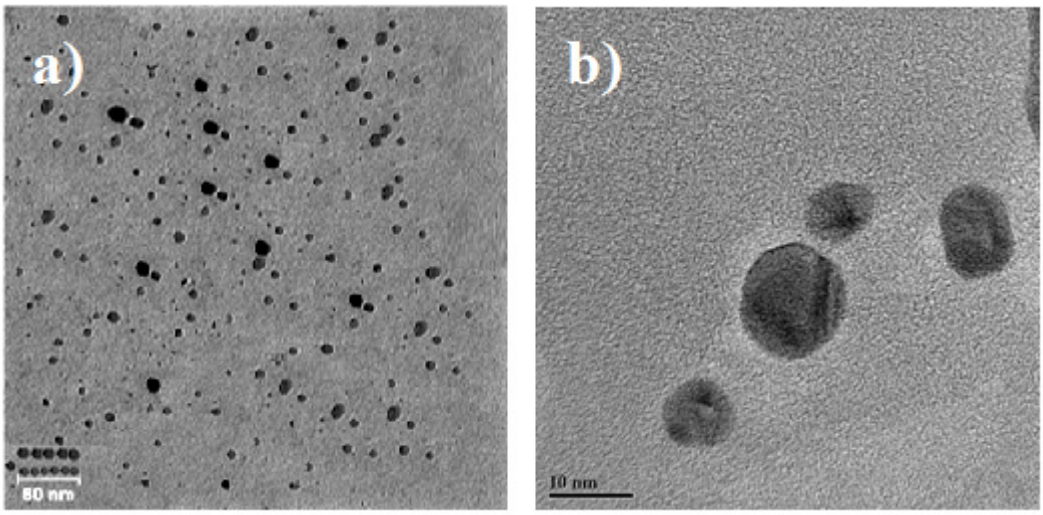

Figs. 2 (a, b). The images of HR TEM for nAF sample.

of HCO_3^- and OH^- (Fig. 3). We have been used to explain the thermal transformation of nAF TG-DTG analysis with reveals some-stage weight loss. At the under 98 °C, about 7.59% weight decreased, which releases O_2, NH_3, H_2 and forms nAF. The weight loss was 2.5%, when the temperature increased from 310 to 500 ºC, which is related to the removal of the remaining acetates in the crystalline nAF. The peak around 103 ºC and a broad peak at 301, 482 ºC, showed acetate of the weight loss of phase transformation to nAF and the removal of adsorbed NH_3 [29, 32].

The FTIR spectrum of $nAlF_3$ has not been showed any Hydroxyl group stretching of water (adsorbed) bands at 3300-3500 cm^{-1} (Fig. 4). The band at 1635-1645 cm^{-1} shows the bending mode of absorbed with a small amount of water, that the nAF has strong affinity for water. Peak observed at 1075 cm^{-1} represents Al–F bending mode [28, 32].

FESEM analysis shows the morphology of synthesized nano sized nAF shown in Fig. 5. The image has been demonstrated spherical particles with agglomeration and has porosity. After the chemical interaction, the synthesized nAF has regular shape having straight fibers connected to each other that indicates the homogeneity and smooth surface of nanoparticle with uniform distribution of particles.

Table 1 demonstration that the bulk density, humidity percent, crystal percent and quality of

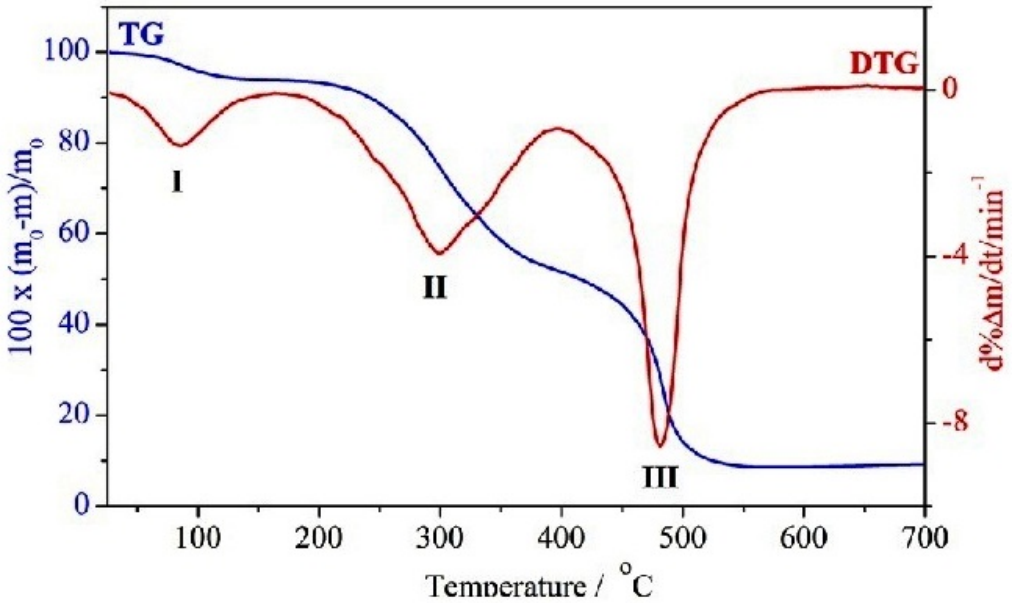

Fig. 3. The TG-DTG curves for nAF dried samples.

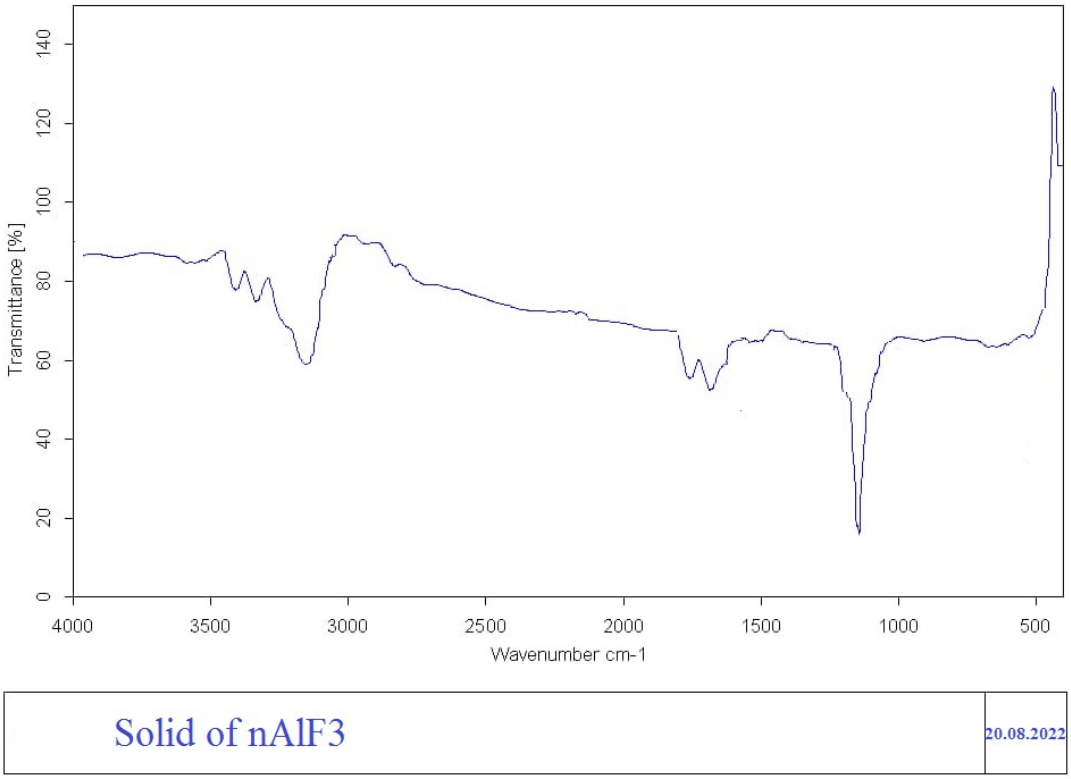

Fig. 4. The FTIR spectrum of the nano AlF_3.

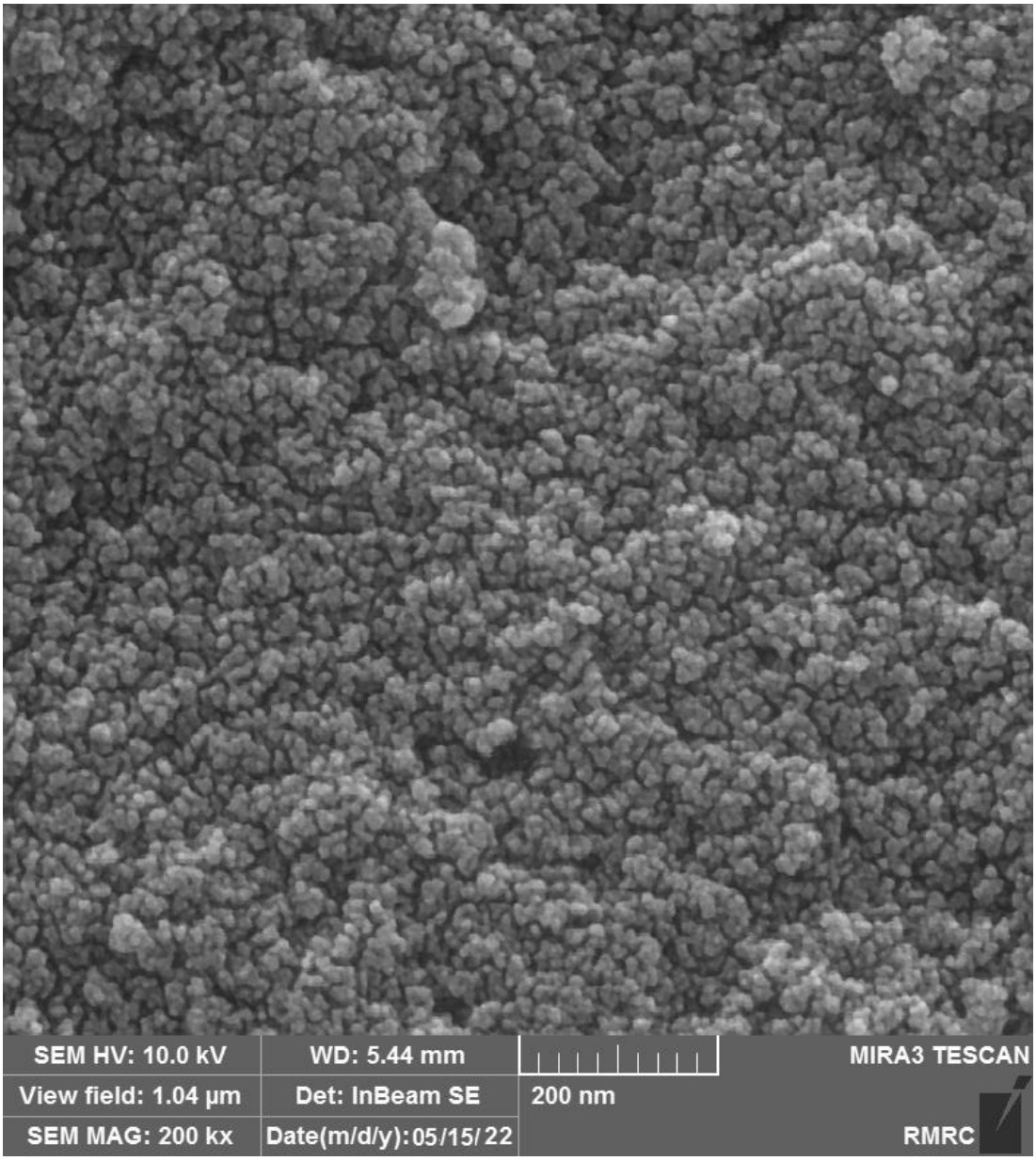

Fig. 5. FESEM images of calcined samples.

nano AlF_3. When increasing precursor gel aging time, the percent of crystal (nAF) increased and then the quality of the crystals improved. The crystal formation can be attributed to the solubility of raw materials together which this is reason of caused homogenized precursor gel. On the other hand, by increasing the time of homogenize the purity of synthesized nAF is increasing and precursor gel the size of crystals was decreased.

The spherical shape of nanoparticles of $ZnAl_2O_4/AlF_3$ (ZA) nanocomposite loaded on PEG is seen in the SEM image (Fig. 6). However, there is an agglomerated between the particles [33, 34].

As indicated in Fig. 7 a, b, after the visible light irradiation exposure, be seen that no serious decolorization is observed, because the Congo red is very stable. In the Fig. 7b with catalyst, we have been seen a decrease in the concentration of Congo red solution. The best result for decolorization of Congo red with $ZnAl_2O_4/AlF_3$ (ZA) nanocomposite has been showed after 90 min with decolorization of 98.9%. A yield of 98.9%

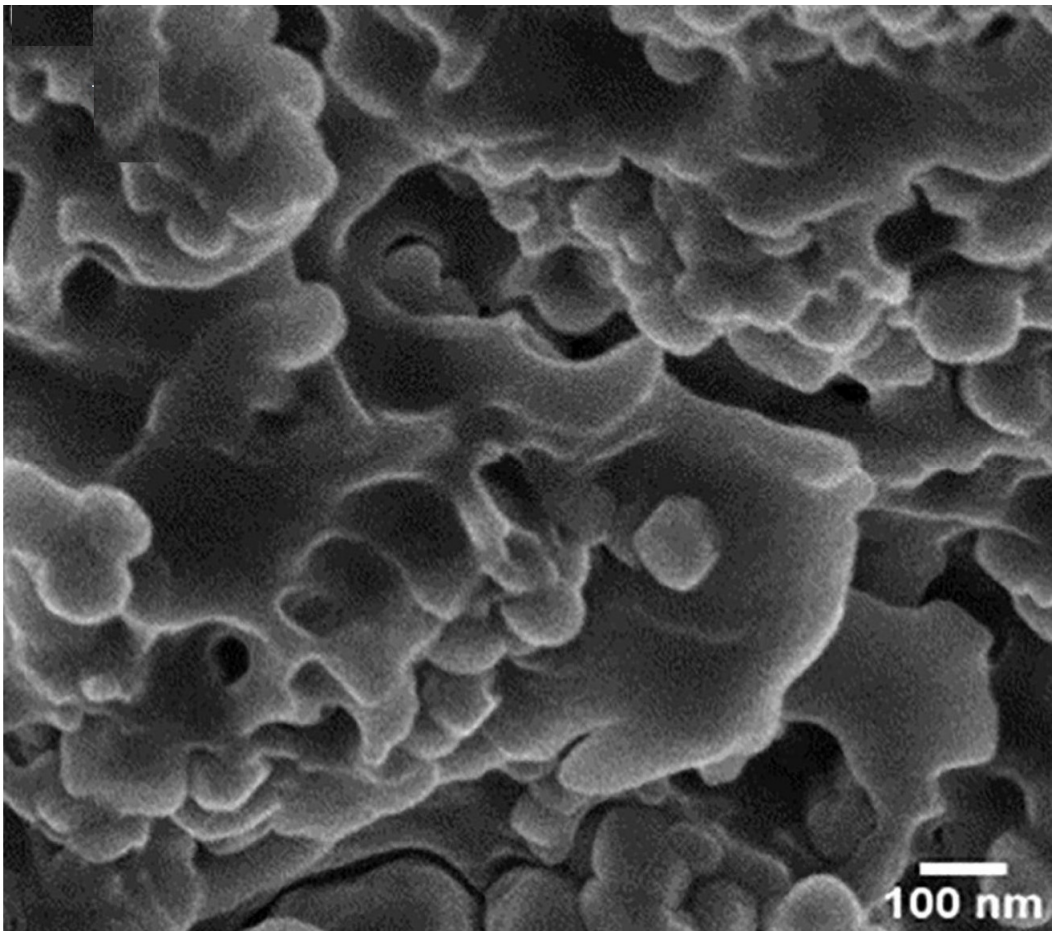

Fig. 6. The SEM image of ZA loaded on PEG.

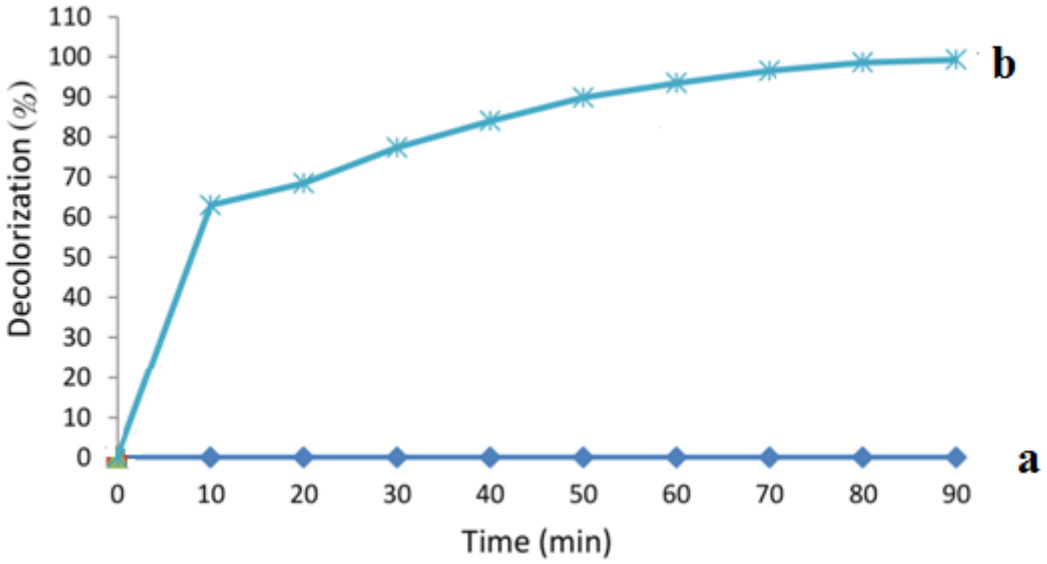

Fig. 7. The rate curve for decolorization of Congo red dye solution using the $ZnAl_2O_4/AlF_3$ (ZA) nanocomposite (under UV light irradiation), (a) without catalyst, (b) with catalyst.

Table 2. Congo Red removal by some of photocatalysts.

	Photo-catalyst	The Pollutant	T(min)	Remov.(%)	Ref.
1	Alg./ C-Fe_2O_3/CdS	20 mg/L	300	91	[35]
2	$ZnFe_2O_4$/Graphene	15 mg/L	270	88	[36]
3	ZnS-CdS	50 mg/L	60	98	[37]
4	$ZnAl_2O_4/AlF_3$	10 mg/L	75	98/9	This work

demonstrated for remove the Congo red, while showed a good efficiency compared with similar researches (Table 2).

CONCLUSIONS

In this study, the nAF and ZA nanocomposite have been synthesized with sol-gel technique and different characterizations have been carried out. Results show that aluminum triisopropylate as Al source for nAF, and nAF is the best source to form the $ZnAl_2O_4/AlF_3$ nanocomposite structure. The particles size of crystals was obtained in 15-20 nm. The XRD pattern of nAF crystals showed high crystallinity and purity in samples and crystal size of sample was 15.6 nm. SEM and TEM analysis showed that the synthesized crystals has spherical shape structure connected to each other, showing the regular shape, the obtained spherical shape regulates the ZA nanocomposite for decolorization of Congo red. The results show the good efficiency of the photocatalyst.

ETHICS APPROVAL AND CONSENT TO PARTICIPATE

Not applicable.

HUMAN AND ANIMAL RIGHTS

No animals/humans were used for the studies that are the basis of this research.

CONSENT FOR PUBLICATION

Not applicable.

AVAILABILITY OF DATA AND MATERIALS

Not applicable.

ACKNOWLEDGMENTS

The financial support and encouragement support was provided by the Research vice Presidency of North Tehran Branch, Islamic Azad University and Executive Director of Iran-Nanotechnology Organization (Govt. of Iran), and Executive Director of Iran-Nanotechnology Organization (Govt. of Iran).

REFERENCES

[1] Leonard, V., (1998), Chemistry of Advanced Materials: An Overview, Wiely-VCH, Inc, Canada, Molecular Precursor Routes to Inorganic Solids. 9: 389-448.

[2] Righini G. C., Pelli S., (1997), Nonlinear properties of semiconductor-doped silica solgel films. J. Sol-Gel Sci. Tech. 8: 991-997. https://doi.org/10.1007/BF02436973

[3] Oda A. M., Kadhum S. H., Farhood A. S., alkadhum H. A., (2014), Degradation of Congo red solution by Zinc Oxide/Silver composite preheated at different temperatures. J. Thermodyn. Catal. 5: 1-5.

[4] Movahedi M., Mahjoub A. R., Janitabar-Darzi S., (2009), Facile synthesis and characterization of CdTiO3 nanoparticles by Pechini sol-gel method. J. Iran. Chem. Soc. 6: 570-577. https://doi.org/10.1007/BF03246536

[5] Elmorsi T. M., Elsayed M. H., Bakr M. F., (2017), Na doped ZnO nanoparticles assisted photocatalytic degradation of congo red dye using solar light. Am. J. Chem. 7: 48-57.

[6] Turner M. E., Trentler T. J., Colvin V. L., (2001), Thin films of macroporous metal oxides. Adv. Mater. 13: 180-183. https://doi.org/10.1002/1521-4095(200102)13:3<180::AID-ADMA180>3.0.CO;2-Y

[7] Aguado J., Serrano D. P., Escola J. M., Garagorri E., Fernandez J. A., (2000), Catalytic cracking of a polyolefin mixture over different acid solid catalysts. Polym. Deg. Stab. 69: 11-16. https://doi.org/10.1016/S0141-3910(00)00023-9

[8] Ouyang J., Zhao Z., Suib S. L., Yang H., (2019), Degradation of Congo red dye by a Fe2O3@CeO2-ZrO2/Palygorskite composite catalyst: Synergetic effects of Fe2O3. J. Colloid and Interf. Sci. 539: 135-145. https://doi.org/10.1016/j.jcis.2018.12.052

[9] Maryani E., Abdullah M., Dayamanti H., Septawendar R., (2016), Effect of ultrasonic irradiation on the characteristic of γ-Al2O3 nanorods synthesized from nitrate salt-starch precursors trough a facile precipitation method. J. Ceram. Soc. Japan. 124: 1205-1210. https://doi.org/10.2109/jcersj2.16158

[10] Amirsalari A., Farjami S., (2015), Effect of pH and calcinations temperature on structural and optical properties of alumina nanoparticles. J. Superlatt. Microstruct. 82: 507-524. https://doi.org/10.1016/j.spmi.2015.01.044

[11] Da-Ros S., Barbosa-Coutinho E., Schwaab M., Calsavara V., Fernandes-Machado N. R. C., (2013), Modeling the effects of calcination conditions on the physical and chemical properties of transition Alumina catalysts. J. Mater. Character. 80: 50-61. https://doi.org/10.1016/j.matchar.2013.03.005

[12] Tayseir Mohammed A. E., Saikat M., (2017), Some studies on the surface modification of sol-gel derived hydrophilic Silica nanoparticles. Int. J. Nano Dimens. 8: 97-106.

[13] Maity S. K., Ancheyta J., Rana M. S., (2005), Support effects on hydroprocessing of maya heavy crude. J. Energy and Fuel. 19: 343-347. https://doi.org/10.1021/ef049732t

[14] Fernandez V. C., Ramrez J., Alejandre A. G., Sanchez-Min-

ero F., Cuevas-Garcıa R., Torres-Mancera P., (2008), Synthesis, characterization and evaluation of NiMo/SiO2-Al2O3 catalysts prepared by the pH-swing method. J. Catal. Today. 130: 337-344. https://doi.org/10.1016/j.cattod.2007.10.101
[15] dao Quan H., Yang H., Tamura M., Sekiya A., (2004), SbF5/PAF-a novel fluorinating reagent in preparing fluorine compounds. J. Fluorine Chem. 125: 1169-1172. https://doi.org/10.1016/j.jfluchem.2004.03.009
[16] Sekiya A., dao Quan H., Tamura M., Gao R. X., Murata J., (2001), Sol-Gel Synthesis and Catalytic Properties of PVC/NiAl2O3/AlF3 nanocomposite. J. Fluorine Chem. 112: 145-148. https://doi.org/10.1016/S0022-1139(01)00483-3
[17] dao Quan H., Tamura M., Takagi T., Sekiya A., (1999), Fluorination of n-dodecane adsorbed on porous aluminium fluoride by gaseous fluorine. J. Fluorine Chem. 99: 167-170. https://doi.org/10.1016/S0022-1139(99)00134-7
[18] Krespan C. G., Dixon D. A., (1996), Fluoroolefin condensation catalyzed by aluminum chlorofluoride. J. Fluorine Chem. 77: 117-126. https://doi.org/10.1016/0022-1139(96)03388-X
[19] Sadjadi M. A. S., Sadeghi B., Meskinfam M., Zare K., Azizian J., (2008), Synthesis and characterization of Ag/PVA nanorods by chemical reduction method. Phys. E: Low-dimens. Syst. Nanostruct. 40: 3183-3186. https://doi.org/10.1016/j.physe.2008.05.010
[20] Sadeghi B., Sadjadi M. A. S., Vahdati R. A. R., (2009), Nanoplates controlled synthesis and catalytic activities of silver nanocrystals. Superlatt. Microst. 46: 858-863. https://doi.org/10.1016/j.spmi.2009.10.006
[21] Sadeghi B., Jamali M., Kia Sh., Amini Nia A., Ghafari S., (2010), Synthesis and characterization of silver nanoparticles for antibacterial activity. Int. J. Nano Dimens. 1: 119-124.
[22] Sadeghi B., Garmaroudi S. F., Hashemi M., Nezhad H. R., Nasrollahi A., Ardalan Si., Ardalan Sa., (2012), Comparison of the anti-bacterial activity on the nanosilver shapes: nanoparticles, nanorods and nanoplates. Adv. Powder Technol. 23: 22-26. https://doi.org/10.1016/j.apt.2010.11.011
[23] Sadeghi B., Pourahmad A., (2012), Synthesis of silver/poly (diallyldimethylammonium chloride) hybride nanocomposite. Adv. Powder Technol. 22: 669-673. https://doi.org/10.1016/j.apt.2010.10.001
[24] Sadeghi B., Ghammamy Sh., Gholipour Z., Ghorchibeigy M., Amini Nia A., (2011), Gold/hydroxypropyl cellulose hybrid nanocomposite constructed with more complete coverage of gold nano-shell. Mic & Nano Lett. 6: 209-213. https://doi.org/10.1049/mnl.2011.0036
[25] Sadeghi B., (2014), Preparation of ZnO/Ag nanocomposite and coating on polymers for anti-infection biomaterial application. Spectrochim. Acta Part A: Molec. Biomolec. Spectros. 118: 787-792. https://doi.org/10.1016/j.saa.2013.09.022
[26] Sadeghi B., (2018), Controlled growth and characterization Ag/ZnO nanotetrapods for humidity sensing. Comb. Chem. High throughput Screen. 21: 1-6. https://doi.org/10.2174/1386207321666180717120417
[27] Sadeghi B., Meskinfam M. A., (2012), A direct comparison of nanosilver particles and nanosilver plates for the oxidation of ascorbic acid. Spectrochim. Acta Part A: Molec. Biomolec. Spectros. 97: 326-328. https://doi.org/10.1016/j.saa.2012.05.082
[28] Liu Ch., Li J., Liew K., Zhu J., Bin Nordin M. R., (2012), An environmentally friendly method for the synthesis of nano-alumina with controllable morphologies. J. RSC Adv. 2: 8352-8358. https://doi.org/10.1039/c2ra20674a
[29] Wuy Y. S., Ma J., Hu F., Li M. C., (2012), Synthesis and characterization of mesoporous Alumina via a reverse precipitation method. J. Mater. Sci. Technol. 28: 572-576. https://doi.org/10.1016/S1005-0302(12)60100-5
[30] Sun X., Li J., Zhang F., Qin X., Xiu Zh., Ru H., (2003), Synthesis of nanocrystalline γ-Al2O3 powders from nanometric ammonium aluminum carbonate hydroxide. J. Am. Ceram. Soc. 86: 1321-1325. https://doi.org/10.1111/j.1151-2916.2003.tb03469.x
[31] Xiuhong M., Linhai D., Xiaohua X., Qiang W., Haiyan W., (2014), Synthesis of macro mesostructured γ-Al2O3 with large pore volume and high surface area by a facile secondary reforming method. J. China Petrol. Process. Petrochem. Technol. 16: 20-28.
[32] Zhu Zh., Sun H., Liu H., Yang D., (2010), PEG-direct hydrothermal synthesis of alumina nanorods with mesoporous structure via AACH nanorod precursors. J. Mater. Sci. 45: 46-54. https://doi.org/10.1007/s10853-009-3886-9
[33] Ramavathu L. N., Tumma B. N., Justin P., (2023), Photocatalytic degradation studies of malachite green dye by hydrothermally synthesized Cobalt Vanadate nanoparticles. Int. J. Nano Dimens. 14: 145-156.
[34] Hossienzadeh Gh., (2023), Innovative fabrication of CeO2 nanoparticles/WO3 nanoplates S-Scheme heterojunction for visible light photocatalytic degradation of nitenpyram insecticide. Int. J. Nano Dimens. 14: 50-59.
[35] Jiang R., Yao J., Zhu H., Fu Y., Guan Y., Xiao L., Zeng G., (2014), Effective decolorization of congo red in aqueous solution by adsorption and photocatalysis using novel magnetic alginate/γ-Fe2O3/CdS nanocomposite. Desali. Water Treat. 52: 238-247. https://doi.org/10.1080/19443994.2013.787551
[36] Jiang R., Zhu H., Fu Y., Jiang S., Zong E., Yao J., (2019), Photocatalytic decolorization of Congo red wastewater by magnetic ZnFe2O4/Graphene nanosheets composite under simulated solar light irradiation. Sci. Eng. 42: 174-182. https://doi.org/10.1080/01919512.2019.1635432
[37] Hadi Fakhri F., Majeed Ahmed L., (2019), Incorporation CdS with ZnS as nanocomposite and using in photo-decolorization of Congo red dye. Indones. J. Chem. 19: 936-943. https://doi.org/10.22146/ijc.38335